Journal of the National Academy of Forensic Engineers®

http://www.nafe.org

ISSN: 2379-3252

DOI: 10.51501/jotnafe.v43i1

Vol. 43 No. 1 June 2026

Wind Damage vs. Storm Surge Damage: Case Studies from Hurricane Helene

By Manuel Matus, PhD, PE, Ziad Azzi, PhD, PE, DFE (NAFE #1343S), and Krishna Sai Vutukuru, PhD, PE, DFE (NAFE #1384M)

Abstract

Between 1980 and 2024, natural hazards have resulted in approximately $2.9 trillion in economic losses across the United States. Tropical cyclones represent the most damaging hazard type, accounting for approximately 53% of total losses, and are classified as multi-hazard events due to the combined impacts of wind loading and storm surge inundation. In the contiguous United States, coastal regions comprise only 10% of the total land area yet contain approximately 40% of the population, making these communities particularly susceptible to damage from hurricane-induced wind as well as storm surge-related forces. Following major events, post-disaster damage assessments conducted by federal agencies (such as FEMA) and by private-sector entities (including insurance carriers) are tasked with distinguishing between wind-related and storm surge-related damage. This forensic differentiation is critical for structural failure analysis, accurate insurance claims adjudication, and equitable allocation of recovery resources. Misattribution can lead to substantial disputes and financial discrepancies. This paper presents a case study for both pre-event vulnerability assessments and post-event forensic evaluations aimed at identifying and differentiating wind-induced versus storm surge-induced damage to residential buildings. The methodology described in this document integrates civil engineering principles and forensic investigation techniques to provide guidance for improving damage attribution accuracy and post-disaster decision-making.

Keywords

Hurricane season, insurance claims, site assessment, wind damage, storm surge damage, forensic engineering

Introduction

Coastal zones, mainly located in the Southeast of the United States and the Gulf of Mexico, constitute inherently multi-hazard environments, where built infrastructure and communities are simultaneously exposed to interacting or sequential natural hazards such as tropical cyclones accompanied by extreme winds, storm surge, and wave loading [1]. In the United States, hurricanes represent one of the most recurrent and destructive hazard agents, generating annual economic losses of tens of billions of dollars [2]. However, individual events can produce far more catastrophic impacts: The 2004-2005 Atlantic hurricane season exceeded $150 billion in total damages [3], and Hurricane Harvey in 2017 incurred losses estimated at more than $100 billion initially [4] — a figure that was later revised to more than $158 billion [5].

Despite the destructive potential of tropical cyclones and severe wind events, flooding remains the costliest weather-related hazard nationwide in terms of property and infrastructure losses [1], [6]. The magnitude of future hurricane- and flood-related impacts is expected to escalate due to population expansion in high-risk coastal regions, shifts in demographic distribution, and the intensification of climate-driven hazards (e.g., hurricanes). Currently, more than half of the U.S. population resides in coastal counties, and long-term projections by the National Oceanic and Atmospheric Administration (NOAA) indicate that these regions will continue to experience high population growth, further amplifying exposure and vulnerability to weather-related hazards [1], [7]-[8].

In recent years, significant advancements have been made in addressing natural hazard design requirements, and code updates have demonstrated measurable benefits. For instance, post-event assessments following Hurricane

Ziad Azzi, PhD, PE, DFE, Director of Engineering, DDA Forensics, Miami, FL, (786) 772-5643, ziad@ddaforensics.com

Ike showed that residences built after 1987, in accordance with the updated standards, exhibited a substantially higher likelihood of structural survival [1], [9]-[11]. In post-hurricane forensic and structural engineering assessments, accurately distinguishing between wind-induced and storm surge-induced structural damage is critical, primarily because insurance coverage frameworks treat these hazards separately. Standard property insurance generally covers wind-related losses while explicitly excluding flood damage, which is instead addressed under dedicated flood-insurance policies.

In such situations, the forensic engineer becomes a focal point in resolving disputes that may arise between insurance carriers and homeowners. As such, it is imperative that the engineering consultants preserve professional independence, exercise unbiased technical judgment, and rigorously apply established engineering methodologies, principles, and standards [12]-[13]. Additionally, because many coastal structures experience complex interactions between wind and surge-related forces during a hurricane, determining the dominant damage mechanism typically requires comprehensive on-site forensic assessments. Such evaluations are especially relevant to forensic engineers, design professionals, insurance adjusters, building code authorities, floodplain managers, and emergency management officials alike, who rely on accurate hazard attribution for technical, regulatory, and financial decision-making to improve current practices [13].

Literature Review

The distinction between wind-induced and storm surge (or flood)-induced damage has evolved into a specialized field within forensic engineering. Historical and recent hurricanes, including Katrina, Ida, Harvey, Irma, Ian, Helene, and Milton, have provided insights into how these forces impact structures, as illustrated by engineering surveys, forensic assessments/reconnaissance, and published literature [14]-[20].

Field surveys after major storms, such as those by the Federal Emergency Management Agency (FEMA), Haag Engineering, and the United States Geological Survey (USGS), reveal that the extent of surge damage is evident from mud/sediment lines, aligned debris, and relatively undisturbed roof and upper wall structures. The timing and sequencing of wind and water impacts documented using NOAA, National Hurricane Center (NHC), FEMA flood maps, and high-resolution aerial/satellite imagery are critical to accurately determine causation. Modern investigations also utilize mobile instrumentation, aerial imagery, and radar, but direct field evidence remains a key factor in determining the cause of damage and discerning whether the failure occurred from excessive wind pressures or from elevated storm surge levels.

On one hand, wind damage commonly follows a top-down progression [9].

- The highest forces (or pressures) are concentrated at roof ridges/corners, eaves, gable ends, and upper wall features, resulting in the removal of claddings, shingles, and occasionally whole roof structures [21]-[25].

- A breach at the roof or walls increases the internal pressure, accelerating the outward force upon building elements and sometimes generating rapid failure of the structure [26]-[29]. It is worthwhile mentioning that ASCE 7-22 [26] directly relates the internal pressure inherent inside a building, depending on the building's classification as enclosed, partially enclosed, open, or partially open. More information on the internal pressure coefficients and the enclosure classification of buildings is available in Chapter 26 of ASCE 7-22 [26].

- The Enhanced Fujita Scale and Saffir-Simpson Hurricane Wind Scale provide empirical correlations between observed building damage and estimated wind speeds, enabling forensics to back-calculate likely wind forces through damage observed during the on-site assessments [30]-[33]. Note that the correlations are very site-specific, and it is highly recommended to cross-check with meteorological data as well as structural analyses.

- Field assessment methods include documenting the presence or absence of debris flow lines or scour at foundations, cataloging damage to windward vs. leeward components, and comparing neighboring structures [34]-[37]. Note that, due to the nature of hurricane winds and their cyclonic rotation, different portions of a building may alternate between windward and leeward conditions over time as the storm translates and winds change direction. Therefore, accurate site-specific meteorological data are key in making field assessments.

On the other hand, surge and flood-related damage commonly follows a bottom-up progression.

- Storm surge exerts hydrostatic (or stationary water) and hydrodynamic (moving water) forces that are vastly greater than those from wind. As a small example, a body of water traveling at 10 feet per second (ft/s) exerts about 200 pounds per square foot (psf) of pressure on a vertical elevation such as a residence wall compared with roughly 25 psf of pressure emanating from 100-mile-per-hour (mph) winds. This assumes a fluid dynamic pressure equal to half the density times the velocity squared, which is a measure of the kinetic energy of the moving fluid per unit volume acting against the wall. Note that, at sea level, the density of water is about 800 times greater than the density of air [26]. Although the respective forces and points of application of water and air fluids on a vertical surface are drastically different, this simple example illustrates how much impact changes in fluid density and velocity can have on the magnitude of hydrodynamic and aerodynamic loading on structures (e.g., wind vs. water flows).

- Characteristic damage includes the undermining of foundations, displacement of entire structures, severe damage to ground-level walls, and evidence of buoyancy (e.g., wood-framed buildings entirely floated off foundations) [34], [36], [38], [39].

- Moving water, wave action, and debris battering typically devastate lower building elements while upper levels may remain relatively undisturbed [40], [41].

- Identification of high-water marks, sediment and debris lines, scoured soil, and comparative analysis of surrounding vegetation/buildings are standard investigative tools [42], [43].

Field Assessment Methodology to Differentiate Wind from Storm Surge Damage

Determining whether structural damage resulted from wind or storm surge is a critical component of post-hurricane forensic assessments. Differentiating between these two mechanisms requires a systematic inspection methodology, informed by the physical characteristics of each peril, the timing and progression of damage, and corroborating climatological and hydrological data.

Site Documentation and Preliminary Observations

Assessment begins with comprehensive site documentation [44], [45]. The forensic engineer should develop a sketch plan noting building orientation, nearby obstructions, water bodies, terrain elevations, and cardinal directions. Evidence of flood levels (such as debris lines, water staining, and sediment marks) should be documented both externally and internally, as evidenced in **Figure 1**. Importantly, flood debris lines identify the maximum inundation height, which, in turn, helps define the application points for wind and water forces in a typical engineering analysis.

High-resolution photographs should capture both overview and close-up details of affected areas. Field notes should identify the material types, construction methods, and the precise elevation of observed damage. This information allows differentiation between zones influenced by wind and those influenced by water, and can also provide valuable information for estimating structural strength and/or gravitational forces. Note that ASCE 7-22 [26]

Figure 1
Flood debris lines: (A) exterior wall and (B) interior column.

provides guidance and guidelines for flood loads, wave loads, and wind loads on structures, as well as load combinations involving the aforementioned in conjunction with other loads. Although the thrust of the paper is to differentiate wind damage from storm surge damage, in reality, the structure experiences a combination of loads from both sources during a severe wind event. As such, one cannot exclude a damage source based solely on visual assessment. Therefore, an analysis involving load combinations is necessary to attribute the degree of damage caused by each source, if applicable.

Wind Damage Indicators

Wind-related damage typically initiates at the upper elevations of a structure, such as the roof, gable ends, and eaves, where aerodynamic uplift forces are greatest and pressure differentials are most pronounced [12], [13], [21]-[23], [38], [46]-[51]. The initial signs of wind distress often include dislodged or uplifted roof coverings, ridge shingles or tiles, and cladding materials, particularly at roof edges and corners where turbulent flow separation occurs. Examples of failed roof covering components are shown in **Figure 2**.

As wind continues to act on the structure, breaches in the building envelope, such as failed roof sheathing or openings in windows and doors, can result in internal pressurization, producing additional outward forces on walls and roof systems that accelerate structural deformation and potential failure of the roof structure. These progressive failures typically manifest as outward displacement of wall assemblies or complete loss of envelope components. Examples of damage to wall assemblies are shown in **Figure 3**. Importantly, the absence of scour,

Figure 2
Failed roof covering components from excessive wind pressures: (A) hip cap shingles and (B) ridge cap tiles.

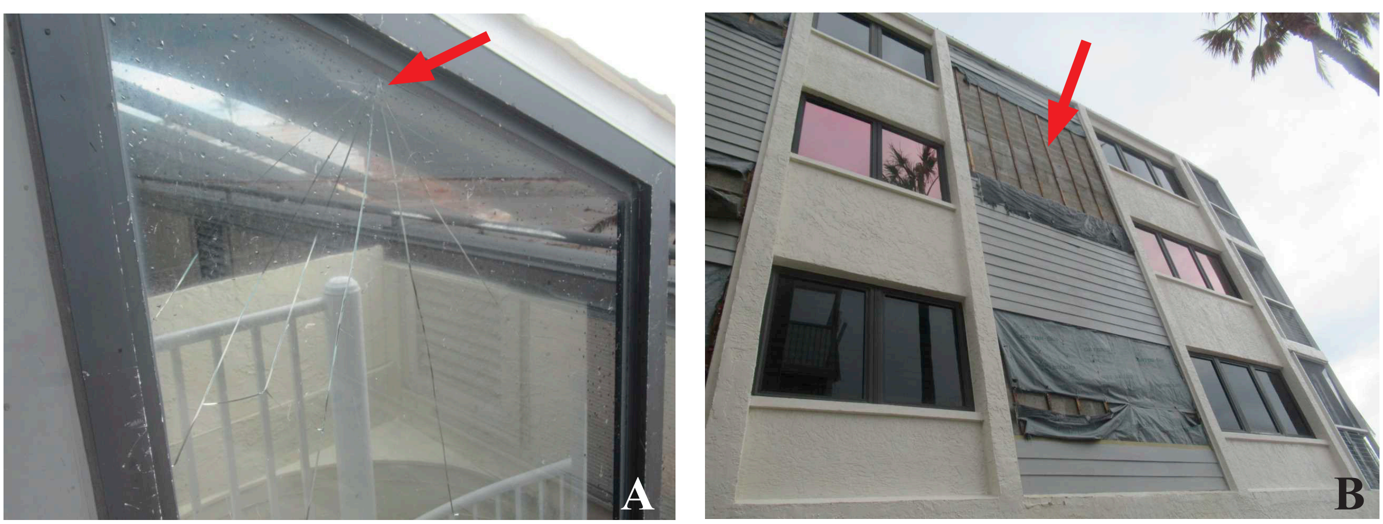

Figure 3
Failed building components: (A) window struck by windborne debris and (B) dislodged wall siding.

sediment deposits, or water staining near the foundation distinguishes damage from wind forces rather than storm surge.

Storm Surge Damage Indicators

Storm surge damage is generally characterized by distress concentrated at the lower portions of a structure, reflecting the powerful hydrostatic and hydrodynamic forces exerted by storm surge and wave action [12], [52]. Typical indicators include severe damage to the lower levels, such as foundation scour, undermining of support systems, and collapse of walls near grade. Evidence of wave impact is often visible in the form of broken cladding, displaced wall panels, or structural deformation occurring near the stillwater level and the wave runup height. Additionally, battering debris can bring down siding components, and walls typically fail with a hinge point, facing the water: the force of the water pushes in the seaward walls, forming a hinge line at the top of the wall. This is opposite the location of the hinge line for wind (which would be the bottom of the wall). Typical examples of storm surge damage to buildings and building components are showcased in **Figure 4**. Note that some of the observations shown in **Figure 4** could be the result of wind damage depending on the severity of the wind event itself and the local climatological conditions including the proximity of the structure to the eye of the storm. However, due to the nature of the failure concentrated toward the lower portion of the elevations, and since wind speeds tend to be minimal near ground level, the likelihood of failure due to severe wind pressures alone is unlikely, unless there is a deficiency in the element or in the connection to its surroundings. As such, a comprehensive forensic assessment coupled

Figure 4
Typical indicators of storm surge damage: (A) toppled masonry wall on ground level, (B) displaced wall siding, (C) seaward wall pushed inward (formation of hinge line at the top of the wall), and (D) battering effects on garage door.

with an engineering analysis is recommended to differentiate the resulting effects of wind and wave pressures.

In many cases, entire buildings exhibit lateral displacement or buoyant uplift of substructures due to the upward and horizontal forces imposed by moving water. Additional diagnostic features include residual debris fields and sediment deposits oriented consistently with the flow direction, which confirm the influence of sustained water movement. Frequently, the upper portions of structures remain intact and are found resting on the ground or transported inland, a condition that strongly indicates buoyant displacement from storm surge rather than progressive wind-induced failure (**Figure 5**). When structures remain standing, damage below the stillwater line or debris line is typically attributed to flooding, while damage above this elevation, without corresponding lower-level distress, suggests wind effects.

Last but not least, structures subjected to intense wave loading action and recurrent impacts from floating debris may experience the failure of load-bearing walls, ultimately leading to partial or total roof collapse. As storm surge waters advance inland, the most severe structural damage typically occurs along the façade directly exposed to the incoming water, where hydrodynamic forces and wave impacts are concentrated. Post-storm reconnaissance studies have consistently documented buildings exhibiting a characteristic “pitched-down” orientation toward the shoreline, indicating that the primary failure mechanism was water-induced loading rather than wind pressure effects [35], [52], [53]. This distinctive structural response is illustrated in **Figure 6**. Notably, the roof covering systems in the remaining sections show little to no evidence of wind-related damage.

Integration of Meteorological and Hydrological Data

The correlating field observations with climatological and hydrological records is critical to establishing event chronology. Meteorological datasets from NOAA, NHC, and USGS should be analyzed to identify the timing and magnitude of peak wind velocities relative to maximum inundation levels [45]. These

Figure 5
Storm surge effects: (A) battering effects on seawall and (B) scouring and erosion of soil below sidewalk.

Figure 6
Aerial photographs: (A) intact building prior to the passing of Hurricane Ian and (B) “pitched down” building after the passing of Hurricane Ian. (Figures courtesy of Eagleview) [54].

incremental datasets allow the assessor to determine whether flooding preceded, coincided with, or followed peak wind events.

In addition, the Post Storm Data Acquisition (PSDA) reports from the National Weather Service (NWS) provide wind speeds, surge stillwater elevations, and measurement annotation results. These data sets are of high importance to help in determining whether the damage was caused by wind and/or storm surge [12], [45]. Similarly, the FEMA Flood Recovery Maps document surveyed waterline elevations and is invaluable for establishing the depth of inundation. As such, forensic engineers must distinguish between stillwater height and total wave height, the latter extending up to 50% to 55% higher than the stillwater level due to wave and debris action. This is illustrated in ASCE 7-22 [26] and shown in **Figure 7**. Note that "ds" is the stillwater level and **Figure 7** contains two diagrams: one with the space behind the vertical wall dry and one where flooding has already occurred in the space behind the vertical wall.

Forensic Correlation and Comparative Analysis

To confirm preliminary conclusions, forensic engineers are highly urged to conduct comparative analysis of surrounding structures and vegetation. The degree of wind-related damage to nearby roofs, trees, and claddings can help estimate local wind intensities. Conversely, uniform low-level destruction or debris patterns aligned with flow direction reinforce the likelihood of surge impact. Even when only the foundation remains, telltale evidence persists. Therefore, determining whether a structure was damaged by wind or storm surge requires a holistic forensic approach combining:

- <u>Damage pattern recognition</u>: Distinguishing between wind and storm surge damage begins with identifying characteristic damage patterns. As noted previously, wind-related damage typically exhibits a top-down progression, with failures initiating at the roof, upper walls, or windward openings as uplift and lateral pressures increase. However, as previously noted, storm surge damage follows a bottom-up pattern, with structural distress starting near the ground or lower elevations due to hydrostatic and hydrodynamic forces, debris impact, and scour.

- <u>Elevation-based analysis</u>: Evaluating the vertical distribution of damage is helpful to establish whether the forces originated from wind or surge-related forces. By comparing observed damage to the elevations, such as documented stillwater levels, debris lines, and high-water marks, forensic engineers can determine if the observed damage aligns with surge-related forces or excessive wind-induced forces. Damage observed below the established flood line is typically associated with storm surge damage (or flooding), whereas damage observed to the higher components of a structure (above the

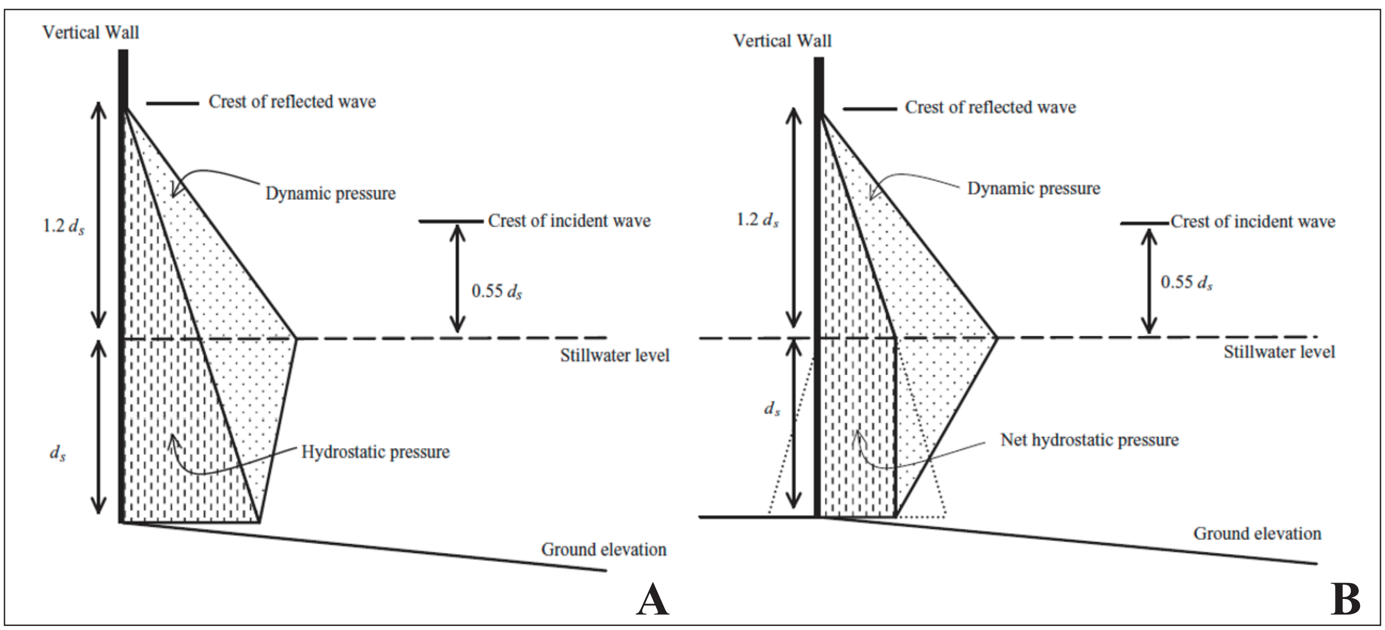

Figure 7
Schematic of breaking wave pressures against a vertical wall: (A) space behind vertical wall is dry and (B) stillwater level is equal on both sides of wall (courtesy of ASCE 7-22 [26], Chapter 5: Flood Loads).

established flood line) is associated with potential impacts from excessive wind-induced forces, if there is any.

- Corroborating Data: Meteorological and hydrological data serve as critical evidence to validate the physical observations obtained during the forensic investigation. Wind speed, predominant wind direction, location of the structure with respect to the eye of the hurricane, location of the hurricane at different times (pre- and post-landfall) are analyzed in conjunction with available nearby tide gauge data, surge hydrographs, and rainfall intensity to establish the timing and magnitude of each hazard. Assessing the structural damage and/or failure with the aforementioned evidence enables a more defensible determination of whether the observed damage corresponds with peak wind loads or the advancing storm surge, or a combination of both.

- Comparative Evaluation: The effect of tropical cyclones can affect vast areas of land simultaneously. Consequently, assessing the damage to neighboring civil infrastructure and vegetation provides valuable contextual evidence. Structures of similar design, elevation, and orientation often exhibit consistent patterns of wind or surge damage under comparable exposure conditions. Additionally, examining fallen trees, displaced debris, and erosion patterns help confirm the dominant force mechanism. This comparative evaluation strengthens forensic conclusions by correlating individual observations with broader, community-scale impact trends, typically associated with tropical cyclones.

In summary, in order to accurately differentiate between wind and surge-related damage, the forensic engineer should document the dimensions of the structure, the location of the structure to obtain flood zones and required base elevations, the roofing components, the wall components, the types of materials that make up the subject structure, the structure's orientation, the damage progression (top-to-bottom or bottom-to-top), flood lines (if any), neighboring structures, surrounding vegetation, and verifiable weather conditions. The forensic engineer should base their findings and conclusions on corroborating that excessive loading, due to wind and surge-related forces, indeed affected the area of the subject structure.

Case Study from Hurricane Helene (2024)

The subject property selected for this case study is located in the city of Keaton Beach, Florida, about 20 miles south of the city of Perry and lies directly along the Gulf of Mexico coastline, facing westward towards the open water. This geographic positioning places the structure in a highly exposed area, classified as Exposure Category D per ASCE 7-22 [26]. The residence itself is a two-story, elevated, wood-framed structure supported by a series of timber posts (or stilts) embedded in the ground, constructed in 1987. The architectural layout includes a partially enclosed lower level, herein referred to as the "first floor," which functions primarily as an open parking and storage area. Approximately 50% of the perimeter of this level is open. The upper level, herein identified as "second floor," is enclosed with conventionally framed wood walls covered with vinyl siding. The roof structure consists of a gable roof type covered with metal panel roof system, as shown in **Figure 8**.

After the passing of Hurricane Helene on September

Figure 8
Front elevation of the residence: (A) prior to Hurricane Helene (courtesy of Google Street View[55] — dated 4/2021) and (B) after the passing of Hurricane Helene (dated 10/2024).

Figure 9
Remnants of stilts used to support the structure before failure (dated 10/2024).

26, 2024, the subject property underwent two post-loss site assessments: the first was conducted by the field adjuster assigned by the insurance company in October 2024, and the second was performed by a forensic engineer in May 2025 as part of a detailed structural evaluation. Findings from both site visits revealed that the entire structure had been completely displaced and removed from its original foundation. No portions of the residential structure remained in situ, as exhibited in **Figure 8**, besides a few limited portions of the stilts that were supporting the main structure in addition to some debris.

The only elements observed at the time of each inspection were the lower segments of the first-floor timber posts, which formerly supported the structure above the ground in accordance with typical coastal elevation practices in addition to a concrete monolithic slab-on-grade. Photographic documentation from both assessments revealed discernible signs of age-related deterioration in the exposed timber elements, including weathering, surface degradation, and biological decay, all consistent with prolonged exposure to moisture (**Figure 9**). Additionally, during the assessment performed by the forensic engineer and his interview with the homeowner, it appears that the structure's exterior cladding system (building envelope) had been upgraded to a vertical board-and-batten finish prior to the reported date of loss.

As the structure itself was no longer present and therefore could not be physically inspected, several dimensional estimates were derived using photographs obtained from publicly available street-level imagery, specifically Google Street View [55]. Based on the visual analysis of these images and the identification of the exterior cladding materials, it was determined that the height of the first-floor, up to the lowest horizontal member of the residence, was "approximately" 7.5 feet above grade. This estimation was derived by identifying the use of standard vinyl siding on the exterior walls, which typically features an exposed height of approximately 5 inches per course. A visual count of the vertically stacked siding sections yielded an estimated total of 18 individual courses, resulting in the calculated overall height. This method, while approximate, provides a reasonable estimate in the absence of direct site measurement, as portrayed in **Figure 10**.

On another note, the subject residence is located within a FEMA-designated "AE" flood zone with a Base Flood

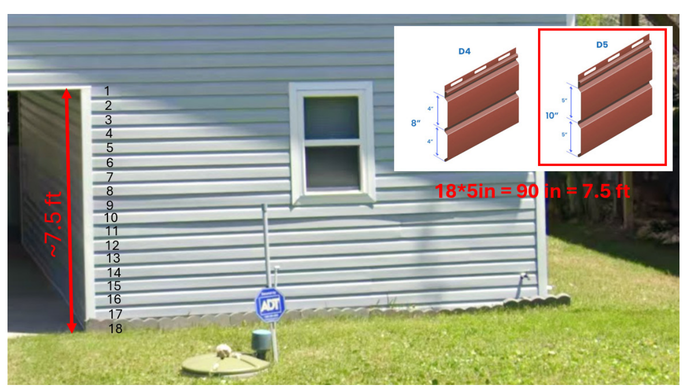

Figure 10
First floor height estimation (about 7.5 feet to lowest horizontal member), courtesy of Google Street View [55] — dated 4/2021.

Elevation (BFE) of 16 feet (EL 16) above NAVD88 datum (North American Vertical Datum of 1988), indicating a coastal high-risk and high-hazard area subject to wave action, storm surge, and velocity flow during major storm events (**Figure 11**).

Note that NAVD88 consists of a leveling network on the North American continent, ranging from Alaska through Canada, across the United States, affixed to a single origin point on the continent. According to FEMA's designation, structures in AE zones are required to have the lowest finished floor elevated at or above the base flood elevation (BFE), allow unobstructed flow of water beneath the building, and use any enclosed area (below the BFE) as parking, building access or storage area only. Being in an area with a BFE of 16 feet, the residence living spaces must be elevated above grade, with the lowest finished floor situated at or above the BFE, in compliance with current floodplain management regulations, regardless of the site's elevation with respect to the mean sea level. Given its location in an AE zone, the residence is particularly vulnerable to storm surge (hydrostatic forces), high-velocity wave impact (hydrodynamic forces), and erosion-related foundation undermining during extreme coastal storm events such as hurricanes. Please note that the structure may have been built following the current standards in the year of the construction of the subject structure. However, based on current FEMA flood elevations, the structure is vulnerable to storm-surge damage.

It must be noted that the BFE is the computed elevation to which floodwater is anticipated to rise during a base flood (a flood having a 1% annual chance of occurrence, also known as the 100-year flood) from the NAVD88 datum. Additionally, the elevation of the structure is estimated to be approximately 7 feet (above NAVD88). As such, the structure's estimated elevation of the second floor, the lowest horizontal structural member (about 7.5 feet above ground level) was insufficient to comply with the regulation provided by the FEMA flood maps (BFE of 16 feet – NAVD88) and did not meet the minimum flood hazard mitigation standards at the time of the date of loss. However, it must be noted that the house was built in the late '80s, and it is possible that it was built for the requirements set forth at the time of the construction of the subject structure.

Hurricane Helene Storm Surge

According to NOAA, Hurricane Helene made landfall in the Big Bend region of Florida on the evening of September 26, 2024, as a Category 4 hurricane according to the Saffir-Simpson Hurricane Wind Scale, bringing severe destruction to coastal communities in the vicinity of the landfall and across the west coast of Florida [57]. Hurricane Helene's path and wind circulation are both presented in **Figure 12**. Furthermore, Hurricane Helene's path made landfall approximately 14 miles northwest of the subject structure as showcased in **Figure 13**, where the yellow pin locates the residence, the red pins locate the position of Hurricane Helene's eye at landfall, and the green

Figure 11
FEMA flood zoning for the subject residence (courtesy of FEMA Flood Maps [56]).

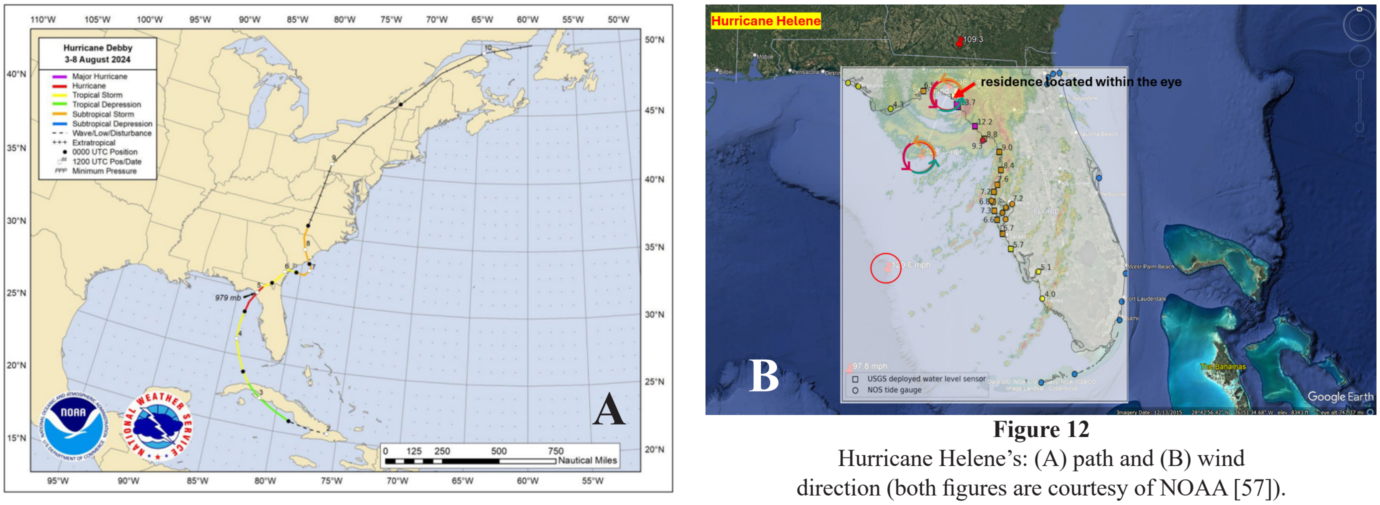

Figure 12
Hurricane Helene's: (A) path and (B) wind direction (both figures are courtesy of NOAA [57]).

pin locates the path of Hurricane Debby (south of the residence). On a side note, Hurricane Debby was a Category 1 hurricane that made landfall near Steinhatchee, Florida, on August 5, 2024. This hurricane and its path were analyzed due to their proximity in terms of time and geographical location at landfall with respect to the subject structure prior to the passing of Hurricane Helene.

Due to the size of Hurricane Helene's wind field along its path, storm surge impacts were amplified across a broad area with effects reaching as far south as Naples and impacting densely populated areas including the Tampa Bay and Sarasota regions. According to data collected by the USGS water level sensor network, the peak surge inundation within the remote stretch between Keaton Beach and Steinhatchee reached 12 to 16 feet above ground level (AGL) as shown in **Figure 13**. It must be noted that the National Hurricane Center storm surge analysis provides water rises Above Ground Level (AGL) measured from the Mean Higher-High Water (MHHW) datum — this is approximately 1.65 ft above NAVD88 datum.

For verification purposes, two independent water level sensors were analyzed to assess storm surge conditions in proximity to the subject property. The first sensor, operated by NOAA at station # 8727520 and located in Cedar Key, Florida, recorded a peak water level rise of approximately 10 feet (**Figure 14**). The graph indicates that the rise in water up to a height of approximately 7.5 feet level occurred on September 26, 2024, at approximately

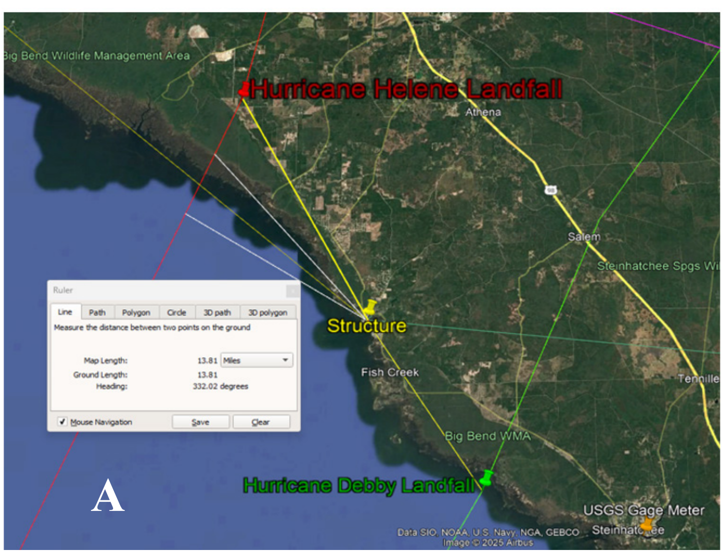

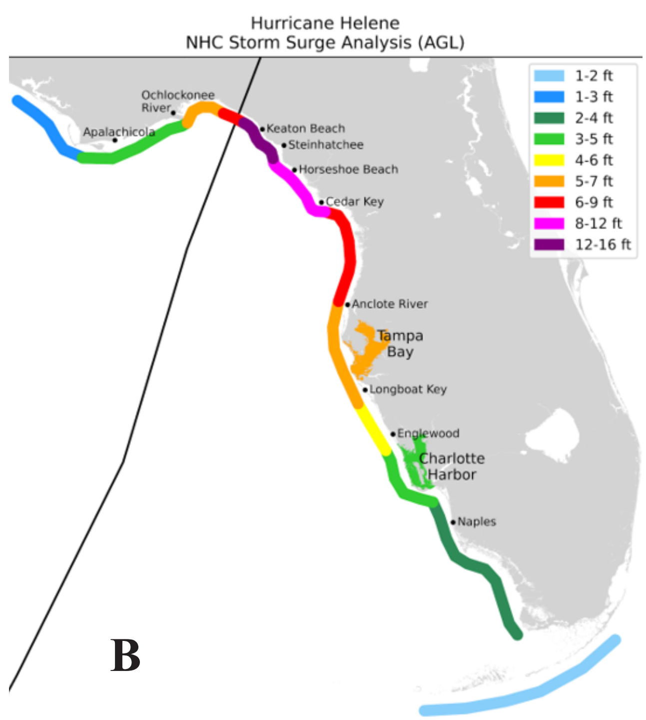

Figure 13
Hurricane Helene's path and landfall with respect to: (A) distance (in miles) to the subject property (courtesy of Google Earth [58]) and (B) storm surge analysis on the west coast of Florida (courtesy of Google [58] and NOAA [57]).

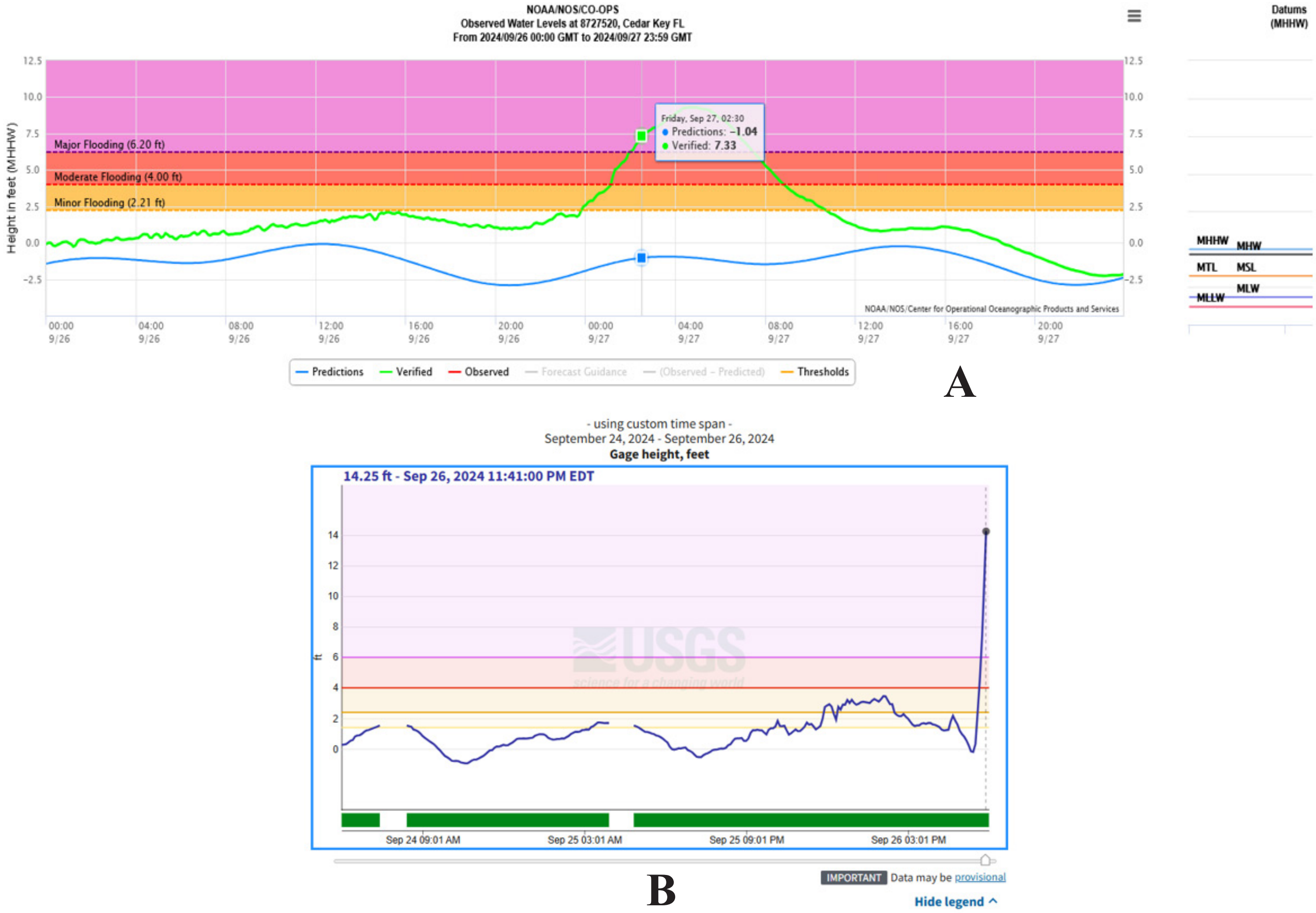

Figure 14
(A) Cedar Key, FL water level (in feet) (NOAA) [59] and (B) Steinhatchee, FL gage height (in feet) (USGS) [60].

9:30 PM (EST). It is important to note that Cedar Key is located approximately 60 miles southeast of the subject property and thus, this sensor may reflect surge behavior in a more southern region of the storm's impact zone. The second sensor, operated by USGS at gage station # 02324170, was located near the Steinhatchee River delta, approximately 15 miles southeast of the subject property. This gauge recorded a peak water level rise of approximately 14 feet before data transmission ceased due to unknown causes (**Figure 14**). The time-history data from this sensor indicated that the water level reached 14.25 feet (above ocean surface mean sea level) at approximately 10:41 PM (EST) on September 26, 2024. The recorded time at which the 14.25-foot water level was reached was used as a reference to estimate when floodwaters were already affecting the lowest horizontal structural member of the subject property, as estimated earlier in **Figure 10**.

Based on the previously discussed data that was collected from the NOAA and USGS sensors and gauges, the approximate sequence of events is outlined as follows:

- The tidal gage at Cedar Key reported water level measurements in GMT. According to the recorded data, the storm surge reached a height of 7.5 feet (above Mean Higher High Water – MHHW) at approximately September 27, 02:30 GMT (or September 26, 21:30 EST). Analysis of the tidal curve indicates that storm surge inundation had already begun prior to the landfall of Hurricane Helene (**Figure 14**). Note that the MHHW datum is defined as the average of the higher high water height of each tidal day observed over the National Tidal Datum Epoch. For stations with shorter series, comparisons of simultaneous observations with a control tide station are made to derive the equivalent datum of the National Tidal Datum Epoch.

- Similarly, data from the Steinhatchee River water level sensor indicated a water level rise reaching 14.25 feet at approximately September 26, 23:41 EDT (or September 26, 22:41 EST). This confirms that the onset of storm surge preceded the hurricane's landfall at this location as well (**Figure 14**).

- In their report [57], the NHC provided the hurricane eye position data in UTC. According to their tracking, the eye of Hurricane Helene was located just offshore on September 27, 00:00 UTC (or September 26, 19:00 EST). Landfall occurred shortly thereafter, with the eye positioned approximately 5 miles inland by September 27, 03:10 UTC (September 26, 22:10 EST).

The previous findings confirm that storm-surge conditions were already underway before Hurricane Helene's official landfall. This indicates that many of the surge-related impacts developed independently of the intense wind forces typically associated with the passage of the storm's eye. Moreover, the observations align with earlier studies showing that surge height is driven more by the storm's overall size and the shallowness of the continental shelf than by pre-landfall wind strength [61], [62]. In particular, long, gently sloping seabeds tend to amplify storm-surge levels, a defining bathymetric feature of Florida's Big Bend region [63].

Hurricane Helene Wind Direction

In the Northern Hemisphere, hurricanes exhibit a counterclockwise rotation due to the Coriolis effect [64]. Throughout Hurricane Helene's approach and eventual landfall, the storm's core remained consistently west of the subject property. As a result, the most intense wind forces affecting the site would have been from the southwest, consistent with the forward-right quadrant of a landfalling hurricane, typically the region associated with the strongest winds and surge impacts. The southwest winds, combined with the concave configuration of Florida's Big Bend coastline, would have funneled water inland in the same general direction as the wind vectors, amplifying storm surge effects along vulnerable low-lying areas, as demonstrated in **Figure 15**. An analysis of wind circulation patterns in the immediate vicinity of the subject property reveals that tangential wind components, around the storm's center, would have directed water and wave energy toward the northeast. This wind-driven water movement would have resulted in significant lateral hydrodynamic forces acting on coastal structures, particularly those with limited elevation and exposure along the Gulf-facing shoreline, such as the subject property. This is portrayed in **Figure 15**.

Based on the estimated wind circulation patterns, tangential wind velocities, and the projected direction of storm surge flow, a targeted survey was conducted to evaluate the displacement and distribution of debris resulting from Hurricane Helene's combined wind- and surge-induced forces. Given the storm's orientation and dynamics, it was anticipated that debris originating from the structures located in Keaton Beach would have traveled in a generally northeast direction, as shown in **Figure 16**. This projected debris path was subsequently validated through

Figure 15
(A) Hurricane Helene circular pattern and (B) Hurricane Helene tangential winds (in yellow) (figures courtesy of Google Earth [58]).

a detailed analysis of high-resolution aerial satellite imagery, which confirmed that the structure had indeed been displaced along the estimated trajectory. Specifically, the entire building was located approximately 1,780 feet northeast of its pre-Hurricane Helene location, aligning with the modeled direction of wind and water forces during the storm event (**Figure 16**).

Displaced Structure

Based on the modeled wind circulation patterns of Hurricane Helene and the estimated direction of storm surge forces described earlier, the main structure was determined to have been displaced approximately 1,780 feet northeast of its original pre-Hurricane Helene location. To conclusively verify that the displaced structure corresponded to the subject property, a detailed visual and dimensional validation was conducted using multiple data sources, including aerial imagery and structural feature comparisons.

The first phase of verification involved analyzing the roof geometry and ventilation layout, features which were not observed in any of the surrounding buildings. As documented in the pre-Hurricane Helene imagery, the subject structure featured a distinctive roof configuration with a rectangular cut-out at the top-left corner, along with three evenly spaced roof vents. These features were found to match those of the displaced structure identified in the October 13, 2024, imagery taken after the passing of Hurricane Helene, strongly supporting the assertion that the same structure had been relocated by storm surge forces, as portrayed in **Figure 17**.

The second phase involved comparing roof area measurements before and after the passing of Hurricane Helene. Satellite imagery dated December 26, 2018, before the alleged date of loss (DOL), and October 13, 2024 (post-DOL), were used to estimate roof square footage. The original structure was found to have a roof area of approximately 1,737 square feet, while the displaced structure measured approximately 2,065 square feet — a difference of roughly 16%. While initially appearing to be a discrepancy, further investigation revealed the source of the additional area. A side-by-side comparison of right-side elevation images of both structures revealed a consistent alignment in architectural features, including window count, placement, and dimensions.

However, a protruding section at the rear elevation of the displaced structure, absent in the earlier satellite imagery, was identified as the cause of the increased roof area (light blue arrows in **Figure 17**). This extension, likely an enclosed or semi-enclosed addition to the rear balcony area noted in the pre-DOL aerial image, appears to have been constructed sometime after the 2018 imagery but prior to the passing of Hurricane Helene. A review of local building permit records yielded no documented approvals for such an addition. Nevertheless, visual evidence strongly suggests that an expansion was made to the rear of the property, as indicated by the green arrow in the pre-DOL imagery. This addition further confirms that the displaced structure matches the architectural characteristics and evolution of the original residence.

To further assess and better understand the magnitude of the forces that the structure was subject to during Hurricane Helene (e.g., wind- and surge-related forces), an estimation of forces was carried out, using engineering analysis and several assumptions, to shed light on the possible mechanisms of failure during the passing of Hurricane Helene.

First, an estimation of the structure's dead load was carried out following assumptions of material self-

Figure 16
(A) Estimated trajectory of debris due to Hurricane Helene forces [58] and (B) satellite image taken on October 13, 2024, after the passing of Hurricane Helene showing original property location and displaced property location (figures courtesy of Eagleview [54]).

weight from ASCE 7-22 (Chapter 3), which resulted in a total dead load of approximately 118 kips. Note this estimation was carried out by considering the roofing material, ceilings, flooring, exterior walls, interior partitions, mechanical-electrical-plumbing (MEP) components and fixed equipment based on the overall dimensions of the

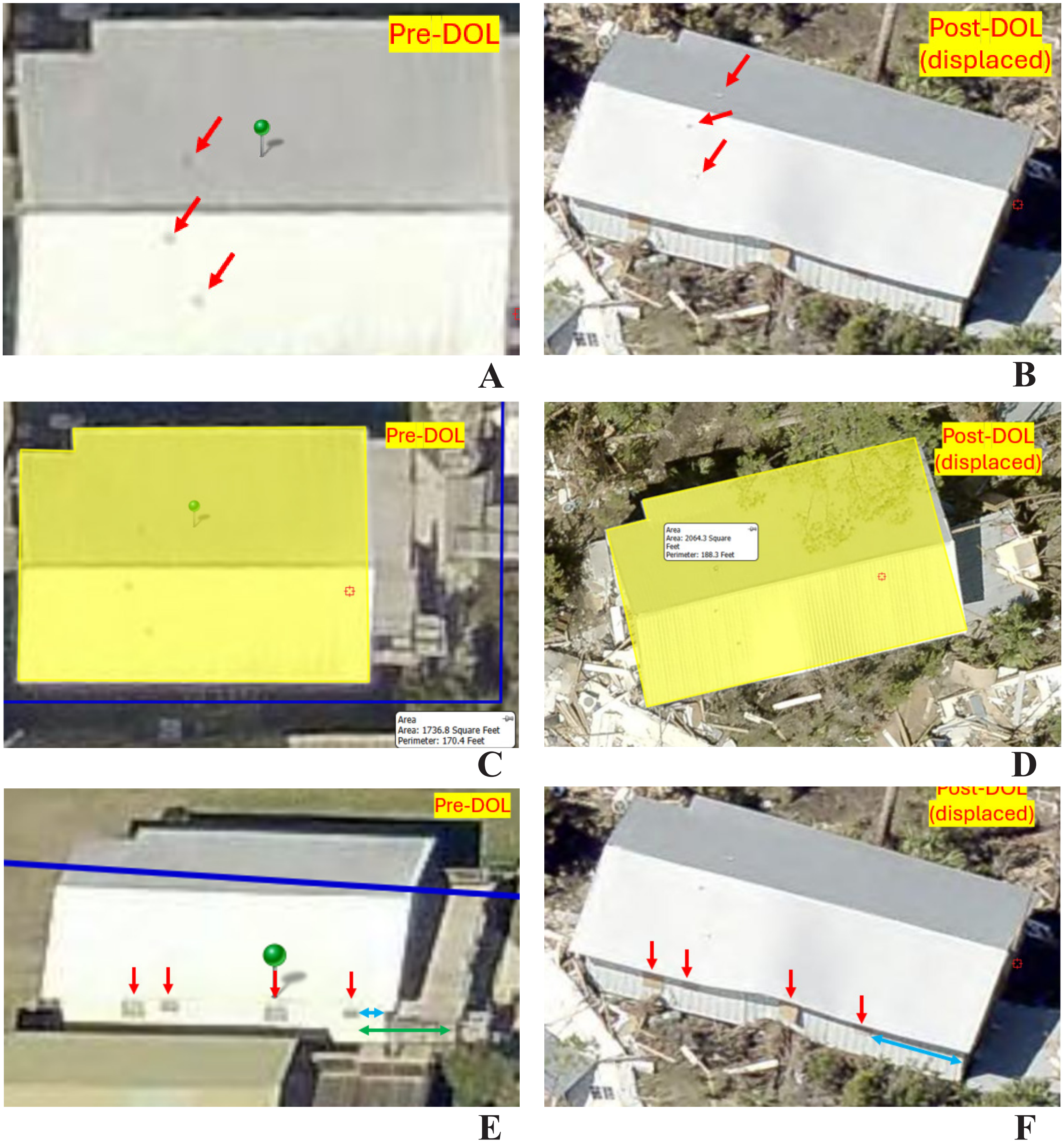

Figure 17

(A) Roof shape and appurtenances pre-DOL, (B) roof shape and appurtenances post-DOL, (C) roof estimated area pre-DOL, (D) roof estimated area post-DOL, (E) south elevation fenestration and details pre-DOL, and (F) south elevation fenestration and details post-DOL (all figures courtesy of Eagleview [54]).

structure (**Figure 18**). Also note that GWB stands for gypsum wall board.

Additionally, attempts to estimate the buoyant forces produced by stillwater onto the structure were estimated and ranged between 605 and 1,142 kips (about 5 to 10 times larger than the self-weight of the structure). This assumption is based on a storm surge height ranging between 12 and 16 feet above ground level, and with a 4.5 to 8.5 feet structure submersion (first-floor height was previously estimated at about 7.5 feet from ground level, and the calculations were conducted for a building with plan dimensions of 60 feet of length and 35 feet of width). Furthermore, the hydrodynamic forces induced on the structure were estimated to be approximately 9.3 kips, assuming a water flow velocity of 5 ft/s. Note that wave impact forces were not estimated [40]. Accordingly, the minimum buoyancy force acting on the structure, assuming about 12 feet of storm surge height, was about five times larger than the building self-weight alone including all the structural and architectural components.

Moreover, following ASCE 7-22 guidelines, the magnitude of the wind-induced forces, assuming 140-mph gusts, was estimated to be approximately 84 kips and 24 kips for lift and drag forces on the structure, respectively. Finally, an estimation of the overturning moment produced by wind-induced forces yielded about 2,600 ft-kip in contrast to the counter-overturning moment produced by the self-weight of the structure, which was estimated as 3,500 ft-kip. A diagram depicting the estimated wind-induced forces and associated overturning moment is shown in **Figure 19**. Note that F1 stands for the windward drag force, F2 is the leeward drag force, F3 stands for the lift force, and W is the associated self-weight of the structure.

Lastly, a visual assessment of the displaced structure revealed the roof covering sustained no discernible signs of missing, torn, displaced or damaged metal panel roofing components, as observed in **Figure 20**. Furthermore, a key finding during the authors' investigation was the deterioration of the columns and metal brackets, which showed clear signs of missing fasteners, wood rot and sectional reduction due to age-related deterioration of the columns/piers.

Based on the analysis of the conditions and the evidence observed at the inspection site discussed earlier, the following conclusions were made:

- The comprehensive forensic analysis of the subject property and the understanding of wind and storm surge effects on structures indicate that the total failure and displacement of the subject structure were caused by excessive storm surge levels and associated hydrodynamic forces, rather than by wind-induced forces. Multiple lines of evidence support this conclusion including structural assessments, engineering analysis, satellite imagery, and the conditions of Hurricane Helene before and after making landfall.

- The aerial imagery of the displaced structure revealed no significant damage to the roof cover-

Component	Dead Load (psf)	Area	Total Load (lbs)
Roof - Metal over Sheathing	10 psf	2,064 SQ FT	20,640
Ceiling - GWB + Joists	8 psf	2,064 SQ FT	16,512
Floor - wood subfloor	10 psf	2,064 SQ FT	20,640
Exterior Walls (wood frame, GWB inside, siding outside)	15 psf	1,508 SQ FT	22,620
Interior Partitions	10 psf	2,064 SQ FT	20,640
Mechanical, Electrical, Plumbing (MEP)	5 psf	2,064 SQ FT	10,320
Fixed Equipment (e.g., cabinets)	3 psf	2,064 SQ FT	6,192
		Total Dead Load (lbs)	**117,564**

Figure 18
Dead load estimates.

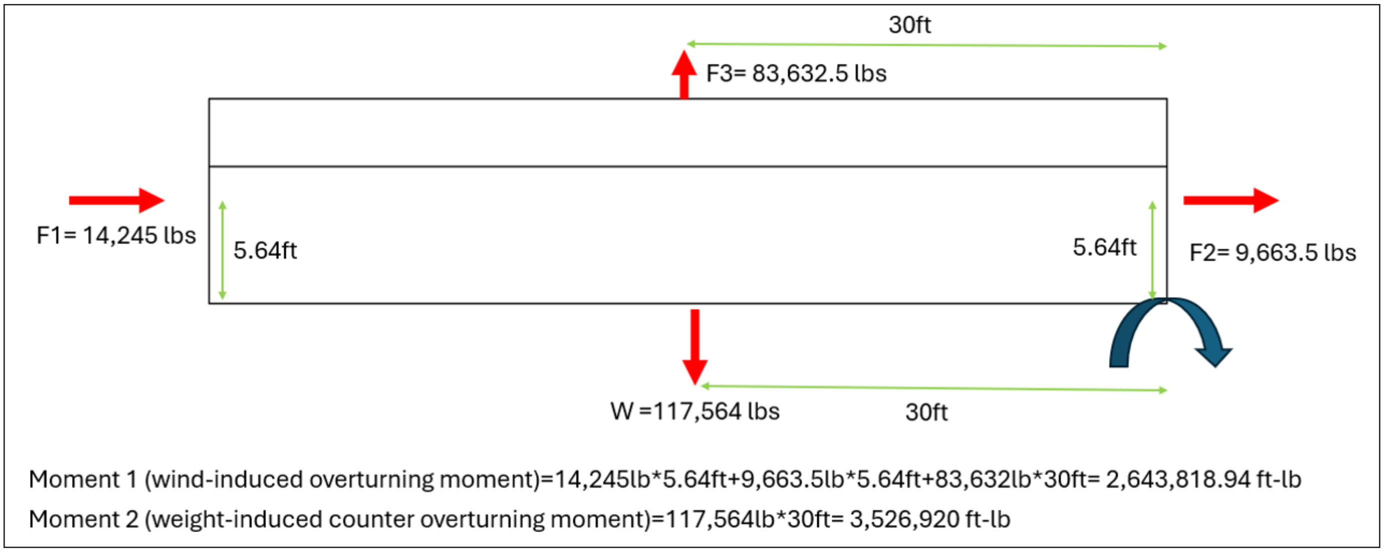

Figure 19
Estimated wind-induced forces diagram and accompanying moment calculations.

Figure 20
Displaced structure —— approximately 1,780 feet northeast from its original location: (A) right elevation view, (B) left elevation view, and (C) top view (all figures courtesy of Eagleview [54]).

ing or exterior siding, components typically susceptible to wind damage, indicating that the structure was not compromised by high wind pressures prior to or after its displacement. The structure was located approximately 1,780 feet northeast of its original location, mostly intact, in a direction consistent with modeled storm surge and tangential wind circulation patterns emanating from the path and trajectory of Hurricane Helene. This displacement aligns with the trajectory predicted by surge-induced water movement rather than chaotic windborne debris behavior.

Other Observations from Hurricane Helene

Although the earlier case study mainly focused on storm surge damage to a coastal structure in the town of Perry, Florida, including the combined effects of hydrostatic and hydrodynamic forces, field investigations of other structures revealed that numerous buildings did survive the elevated storm surge levels recorded at the time of the passing of Hurricane Helene. Such structures were noted with distinct wind-related damage as shown earlier in the manuscript. It was determined that a key factor in these structures withstanding the storm was their relatively recent construction, which followed updated versions of the local jurisdiction and state building codes. The assessment of the neighboring structures included obtaining permit histories and property appraiser reports, providing information pertaining to their year of construction as well as any recent roof replacement permits. This section summarizes the mechanisms of wind-induced damage observed in these surrounding structures and contrasts them with the damage patterns associated with storm surge.

Wind-induced damage during hurricane events is primarily driven by aerodynamic pressures acting on the building envelope and roof system. These pressures result from a combination of sustained wind flow, gust effects, turbulence, and flow separation around building geometries due to bluff-body aerodynamics. Elevated structures located outside the storm-surge inundation zone remain vulnerable to these forces, particularly at building corners, roof edges, ridges, and discontinuities in the envelope [50], [51], [65]. Additionally, due to the atmospheric boundary layer profile, structures with higher elevations have increased resiliency against surge-related forces but are exposed to increased wind-induced loading. Greater elevations result in increased forces to the lateral force resisting systems, such as foundation columns, imposing increased moment loading that the columns and their bracing connections must withstand, signifying an important aspect of the structure to analyze.

Suction (negative) pressures acting on roof coverings can exceed the attachment capacity of shingles, tiles, membrane systems as well as wall components leading to localized loss of roof or envelope covering materials. Once roof and/or wall coverings are compromised, increased internal pressurization may occur if envelope breaches develop, further amplifying uplift forces and accelerating progressive failure of the structure. Windborne debris impacts may additionally contribute to envelope breaches, particularly at wall claddings, soffits, fenestration systems, and garage doors [21].

As such, typical wind damage observations included partial loss of roof coverings, displaced or uplifted shingles, cracked or detached wall cladding, and damage to soffits as well as fascia boards. These damaged areas were generally localized in wind-critical zones and exhibited directional characteristics aligned with the prevailing wind field during the event.

The contrast between wind-induced damage in elevated structures and storm-surge–dominated damage in low-lying structures is significant for forensic attribution. Storm surge damage is characterized by lateral displacement of structural components, collapse or flotation of walls and floors, erosion or scour at foundations, and widespread water intrusion with associated sediment and debris patterns. In comparison, wind damage is generally more selective, affecting envelope components and roof systems without producing global structural instability in properly elevated buildings, as exhibited in **Figure 21** [21], [38], [48], [66]-[74].

The co-existence of these damage modes within the same geographic region underscores the importance of elevation, exposure, and load path continuity in determining damage causation. While both wind and storm surge are generated by the same meteorological event, the resulting damage mechanisms are distinct and must be evaluated independently to ensure accurate forensic conclusions. Representative photographs of wind-induced damage to elevated structures are included to illustrate typical envelope and roof failures attributable to aerodynamic loading (**Figure 22**). These photographs document roof covering displacement, localized wall cladding damage, and envelope breaches consistent with wind action, providing a visual contrast to the storm-surge–driven damage presented in the primary case study. More information on wind flow around buildings as well as wind-related damage to residential roofs including shingle and tile roof coverings can be found in Azzi et al. [21].

Conclusion

Understanding the mechanisms by which hydrostatic and hydrodynamic loads interact with structural systems enables forensic engineers to more precisely differentiate

Figure 21
Coastal structure exhibiting: (A) warping of roof covering and (B) detachment of wall cladding.

Figure 22
Observed wind damage: (A) dislodging of metal panels in high suction pressure zones, (B) torn and partially torn shingles, (C) dislodging of soffits and roof fascia boards, and (D) warping of metal panels.

wind-induced damage from water-induced damage, mainly elevated storm surge levels. Hydrostatic and hydrodynamic actions primarily degrade structural elements at or near the foundation by inducing uplift, scour, and lateral fluid pressures. In contrast, wind loads produce their highest demand at elevated components such as roof coverings and components because wind velocity and corresponding aerodynamic pressures increase with height above the ground. Moreover, due to the substantially higher density of water relative to air (800:1), moving water can impart significantly greater momentum and lateral forces on structural members than wind, as shown in the aforementioned calculations section. Therefore, it is essential to accurately differentiate between wind and surge/flood damage in structural forensic investigations for the following reasons:

- Wind and flood damage are often differently insured. Establishing the correct peril is critical for fair claim resolution and policy compliance.

- Understanding the nature of damage informs future engineering standards and code compliance. For wind, this might include reinforced envelope components and impact-resistant fenestration design. On the other hand, for storm surge, strategies include increased elevation, foundation retrofitting, and breakaway construction in lower elevations of the property.

- Building codes and FEMA standards often rely on forensic assessments after the passing of extreme events to mandate peril-specific construction techniques in relevant geographical areas.

- Accurate assessment of wind versus storm surge damage guides emergency planning, regional development, and infrastructure upgrades.

- Urban planners, FEMA associates, and state agencies use forensic data to guide hazard mapping, land-use planning, and community resilience initiatives. Understanding true loss causation supports smarter investment in infrastructure and life-safety upgrades.

- Erroneous determination of causation can lead to unsafe reconstruction, legal disputes, and long-term vulnerability of coastal structures and communities.

Accurately distinguishing between wind and surge damage ensures technical, legal, financial, and ethical credibility in the aftermath of catastrophic storms. Literature, case studies, and expert practice all converge on the necessity of a rigorous, evidence-driven approach that protects property owners, supports infrastructure resilience, and maintains the credibility of the engineering discipline in general and the forensic engineering discipline in particular.

Acknowledgments

The authors greatly acknowledge the internal support provided by DDA Forensics and the engineering team. The contents of this paper reflect the views of the authors, who are responsible for the facts and the accuracy of the information presented herein.

References

[1] H. Masoomi, J. van de Lindt, M. Ameri, T. Do and B. Webb, “Combined Wind-Wave-Surge Hurricane-Induced Damage Prediction for Buildings,” ASCE Journal of Structural Engineering, vol. 145, no. 1, 2018.

[2] M. Baradaranshoraka, J. Pinelli, K. Gurley, X. Peng and M. Zhao, “Hurricane Wind versus Storm Surge Damage in the Context of a Risk Prediction Model,” ASCE Journal of Structural Engineering, vol. 143, no. 9, 2017.

[3] R. Pielke Jr., J. Gratz, C. Landsea, D. Collins, M. Saunders and R. Musulin, “Normalized Hurricane Damage in the United States: 1900–2005,” ASCE Natural Hazards Review, vol. 9, no. 1, 2008.

[4] K. Quealy, “The Cost of Hurricane Harvey: Only One Recent Storm Comes Close," The New York Times, 1 September 2017. [Online]. Available: https://www.nytimes.com/interactive/2017/09/01/upshot/cost-of-hurricane-harvey-only-one-storm-comes-close.html?smid=pl-share. [Accessed 25 November 2025].

[5] N. D. O. Commerce, “Hurricane Harvey: A Look Back Seven Years Later,” National Environmental Satellite, Data, and Information Service, 26 August 2024. [Online]. Available: https://www.nesdis.noaa.gov/news/hurricane-harvey-look-back-seven-years-later. [Accessed 25 November 2025].

[6] NOAA, "National Coastal Population Report: Population Trends from 1970 to 2020," National Oceanic and Atmospheric Administration, 2017.

[7] K. Crosset, T. Culliton, P. Wiley and T. Goodspeed, "Population trends along the coastal United States 1980-2008," National Oceanic and Atmospheric Administration (NOAA), Washington, DC, 2004.

[8] NOAA, "Natural hazard statistics," National Oceanic and Atmospheric Administration, 2017.

[9] M. McCullough, A. Kareem, A. Donahue and J. Westerink, "Structural damage under multiple hazards in coastal environments," Journal of Disaster Research, vol. 8, no. 6, pp. 1042-1051, 2013.

[10] T. Tomiczek, A. Kennedy and S. Rogers, "Collapse Limit State Fragilities of Wood-Framed Residences from Storm Surge and Waves during Hurricane Ike," ASCE Journal of Waterway, Port, Coastal, and Ocean Engineering, vol. 140, no. 1, 2013.

[11] FEMA, "Mitigation Assessment Team Report: Hurricane Ike in Texas and Louisiana," Federal Emergency Management Agency (FEMA), Washington, DC, 2009.

[12] D. Teasdale, "Field Evaluation of Damage from Wind and Flooding," in Structures Congress 2008: Crossing Borders, 2008.

[13] E. Roberts, "A Guide to Wind Versus Water Assessments for Property Damage Claims," J.S. Held LLC, 2022.

[14] NIST, "Performance of Physical Structures in Hurricane Katrina and Hurricane Rita: A Reconnaissance Report," National Institute of Standards and Technology, NIST Technical Note 1476, 2006.

[15] D. Prevatt, S. Kameshwar, D. Roueche, B. Rittelmeyer, T. Duarte, T. Heo, H. Ibrahim, S. Klepac, O. Lafontaine, T. Lin, L. Manuel, S. Pilkington, Y. Pinyochotiwong, J. Santiago-H, S. Strader, K. Gurley, T. Kijewski-Correa and K. Mosalam, "JOINT PRELIMINARY VIRTUAL AND EARLY ACCESS RECONNAISSANCE REPORT (PVRR-EARR)," National Science Foundation, Structural Extreme Events Reconnaissance (StEER), 2021.

[16] NHC, "Tropical Cyclone Report: Hurricane Harvey," National Hurricane Center, 2018.

[17] FEMA, "Hurricane Irma in Florida: Building Performance Observations, Recommendations, and Technical Guidance," Federal Emergency Management Agency, Mitigation Assessment Team Report, FEMA P-2023, 2018.

[18] M. Cortes, P. Arora, L. Ceferino, H. Ibrahim, D. Istrati, D. Reed, D. Roueche, A. Safiey, T. Tomiczek, I. Zisis, M. Alam, T. Kijewski-Correa, D. Prevatt and I. Robertson, "StEER: Hurricane Ian Preliminary Virtual Reconnaissance Report (PVRR)," Structural Extreme Events Reconnaissance (StEER) - Hurricane Ian, DesignSafe-CI, 2022.

[19] A. Kyprioti, J. Yuzbasi, H. Dang, A. Jana, S. Kameshwar, A. Diekmann, S. Garcia, P. Mohammadi, M. Gutierrez Soto, B. Webb and e. al., "EARLY ACCESS VIRTUAL RECONNAISSANCE REPORT (EARR)," National Science Foundation (NSF), Structural Extreme Events Reconnaissance (StEER), 2025.

[20] T. Do, W. Wang, M. Amini, A. Abdelhady, S. Xu, R. NEGRI, S. Kameshwar, C. Wang, H. Dang, A. Jana, E. Carter, M. Alam, T. Kijewski-Correa, D. Prevatt, D. Roueche and K. Wolohan, "StEER: Hurricane Milton Preliminary Virtual Reconnaissance Report (PVRR)," National Science Foundation (NSF), Structural Extreme Events Reconnaissance (StEER) - Hurricane Milton, DesignSafe-CI, 2025.

[21] Z. Azzi, K. Vutukuru and M. Matus, "Discerning Wind-related Damage to Residence Roofs," Journal of the National Academy of Forensic Engineers, 990, 2026.

[22] Z. Azzi, F. Habte, A. Elawady, A. Chowdhury and M. Moravej, "Aerodynamic Mitigation of Wind Uplift on Low-Rise Building Roof Using Large-Scale Testing," Frontiers in Built Environment, vol. 5, no. 149, 2020.

[23] Z. Azzi, F. Habte, K. S. Vutukuru, A. G. Chowdhury and M. Moravej, "Effects of roof geometric details on aerodynamic performance of standing seam metal roofs," Engineering Structures, vol. 225, no. 111303, 2020.

[24] C. Feng, A. Chowdhury, A. Elawady, D. Chen, Z. Azzi and K. Vutukuru, "Experimental assessment of wind loads on roof-to-wall connections for residential buildings," Frontiers in Built Environment, vol. 6, no. 10, 2020.

[25] K. Alawode, K. Vutukuru, A. Elawady and A. Chowdhury, "Review of wind loading on roof to wall connections in low-rise light wood-frame residential buildings," Journal of Wind Engineering and Industrial Aerodynamics, vol. 236, no. 105360, 2023.

[26] ASCE/SEI-7, Minimum Design Loads and Associated Criteria for Buildings and Other Structures, Reston, VA, USA: American Society of Civil Engineers (ASCE), 2022.

[27] K. Vutukuru, M. Moravej, A. Elawady and A. Chowdhury, "Holistic testing to determine quantitative wind-driven rain intrusion for shuttered and impact resistant windows," Journal of Wind Engineering and Industrial Aerodynamics, vol. 206, 2020.

[28] K. Vutukuru, M. Moravej and A. Chowdhury, "Wind driven rain intrusion reduction for shuttered windows," in Proceedings of 15th International Conference on Wind Engineering (15ICWE), Beijing, China, 2019.

[29] K. Vutukuru, J. Erwin and A. Chowdhury, "Full-scale simulation of wind-driven rain and a case study to determine the rain mitigation effect of shutters," Wind & Structures, vol. 38, no. 3, pp. 171-191, 2024.

[30] T. Fujita, "Proposed characterizations of tornadoes and hurricanes by area and intensity," SMRP 91, 1971.

[31] J. McDonald, K. Mehta, D. Smith and J. Arn Womble, "The Enhanced Fujita Scale: Development and Implementation," in ASCE Forensic Engineering 2009: Pathology of the Built Environment, 2009.

[32] H. Saffir, "Hurricane Wind and Storm Surge," The Military Engineer, vol. 423, pp. 4-5, 1973.

[33] R. Simpson, "The Hurricane Disaster Potential Scale," Weatherwise, vol. 27, no. 169, pp. 169-186, 1974.

[34] T. P. Marshall, E. Brusky and J. Last, "Storm surge on Lake Butte des Morts during the 11 June 2001 bow echo event," in 21st Conference on Severe Local Storms, San Antonio, TX, 2002.

[35] FEMA, "Is it Wind or Water?" Federal Emergency Management Agency 46, 1989.

[36] T. Marshall, "Hurricane Ivan Damage Survey," in 27th Conference on Hurricanes and Tropical Meteorology, Monterey, CA, 2006.

[37] FEMA, "Hurricane Ivan in Alabama and Florida: Observations, Recommendations, and Technical Guidance," Federal Emergency Management Agency, Mitigation Assessment Team Report, 294, 2005.

[38] T. Marshall, W. Bunting and J. Wiethorn, "Procedure for assessing wind damage to wood-framed residences," in The Symposium on the Fujita Scale and Severe Weather Damage Assessment, 83rd Annual Meeting, Long Beach, CA, 2003.

[39] FEMA, "Hurricane Katrina in the Gulf Coast," Mitigation Assessment Team Report: Building Performance, Observations, Recommendations, and Technical Guidance, FEMA 549, 2006.

[40] FEMA, "Coastal Construction Manual: Principles and Practices of Planning, Siting, Designing, Constructing, and Maintaining Residential Buildings in Coastal Areas (Fourth Edition)," Federal Emergency Management Agency, FEMA P-55, 2011.

[41] A. Ewis and O. Nofal, "Leveraging national datasets for systematic socio-physical coastal flood risk assessment at the community level," Computer-Aided Civil and Infrastructure Engineering, vol. 40, no. 25, pp. 4132-4148, 2025.

[42] USGS, "Field manual for identifying and preserving high-water mark data," United States Geological Survey, 2017.

[43] T. Koenig, J. Bruce, J. O'Connor, B. McGee, R. Holmes, R. Hollins, B. Forbes, M. Kohn, M. Schellekens, Z. Martin and M. Peppler, "Identifying and preserving high-water mark data," United States Geological Survey, 2016.

[44] FEMA, "Flood Damage-Resistant Materials Requirements for Buildings Located in Special Flood Hazard Areas in accordance with the National Flood Insurance Program," Federal Emergency Management Agency (FEMA) Technical Bulletin 2, 2008.

[45] D. Peraza, W. Coulbourne and M. Griffith, Engineering Investigations of Hurricane Damage: Wind versus Water, American Society of Civil Engineers (ASCE), ISBN: 9780784413715, 2014.

[46] A. Mehrabi, S. Dolati, P. Malla, S. Farhangdoust and Z. Azzi, Non-destructive Testing for Inspection of Bridges and Buildings, Cambridge Scholars Publishing, ISBN: 9781036445287, 2025.

[47] Z. Azzi, H. Al Sayegh, O. Metwally and M. Eissa, "Review of Nondestructive Testing (NDT) Techniques for Timber Structures," Infrastructures, vol. 10(2), no. 28, 2025.

[48] A. Tolera, K. Mostafa, A. Chowhudry, I. Zisis and P. Irwin, "Study of wind loads on asphalt shingles using full-scale experimentation," Journal of Wind Engineering and Industrial Aerodynamics, vol. 225, 2022.

[49] F. Habte, M. Mooneghi, T. Baheru, I. Zisis, A. Chowdhury, F. Masters and P. Irwin, "Wind loading on ridge, hip and perimeter roof tiles: A full-scale experimental study," Journal of Wind Engineering and Industrial Aerodynamics, vol. 166, pp. 90-105, 2017.

[50] M. Matus, "Low-rise Irregular Shaped Buildings," FIU Electronic Theses and Dissertations, 5410, 2023.

[51] M. Matus and I. Zisis, "Wind-induced Pressure Distribution on Non-rectangular Shaped Low-rise Buildings," ASCE Journal of Structural Engineering (In production), 2025.

[52] T. Marshall, "Storm Surge Damage to Buildings," Haag Engineering Co., 2014.

[53] T. Marshall, "Hurricane Katrina Storm Damage Survey," Haag Engineering Co., Carrollton, Texas, 2005.

[54] Eagleview, "ConnectExplorer Pictometry Aerial Imagery," 13 October 2024. [Online]. Available: https://explorer.eagleview.com/index.php. [Accessed August 2025].

[55] Google, "Street View digital images, Google Maps," April 2021. [Online]. Available: https://maps.google.com. [Accessed August 2025].

[56] FEMA, "FEMA Flood Maps," 9 January 2025. [Online]. Available: https://hazards-fema.maps.arcgis.com/apps/webappviewer/index.html. [Accessed August 2025].

[57] NHC, "TROPICAL CYCLONE REPORT: HURRICANE HELENE," National Hurricane Center, 2025.

[58] Google, "Earth View digital images, Google Earth," 2025. [Online]. Available: https://earth.google.com/web/. [Accessed August 2025].

[59] NOAA, "NOAA Tides & Currents," [Online]. Available: https://tidesandcurrents.noaa.gov. [Accessed August 2025].

[60] USGS, "Streamflow Measurements for the Nation," [Online]. Available: https://waterdata.usgs.gov/nwis/measurements. [Accessed August 2025].

[61] G. Haddow, J. Bullock and D. Coppola, "Chapter 2: Natural and Technological Hazards and Risk Assessment," in Introduction to Emergency Management (Sixth Edition), Elsevier, 2017, pp. 33-77.

[62] H. Needham and B. Keim, "Correlating Storm Surge Heights with Tropical Cyclone Winds at and before Landfall," Earth Interactions, American Meteorological Society, vol. 18, pp. 1-26, 2014.

[63] R. Mattson, T. Frazer, J. Hale, S. Blitch and L. Ahijevych, "Florida Big Bend," in Seagrass Status and Trends in the Northern Gulf of Mexico: 1940–2002, USGS, 2007.

[64] R. Smith and M. Montgomery, Tropical Cyclones: Observations and Basic Processes, Elsevier, 2023.

[65] H. Sarma, M. Matus, S. Lee and I. Zisis, "Influence of Building Shape-factor on Wind Loads for Non-Rectangular Low-Rise Structures," Journal of Building Engineering, vol. 120, no. 115314, 2026.

[66] H. Snoke, "Asphalt-prepared roll roofings and shingles," National Bureau of Standards, Report BMS70, 1941.

[67] L. Sharara, J. Jordan and R. Kimble, "Residential Roofing Evaluation," in Fifth Forensic Engineering Congress, Washington, D.C., USA, 2009.

[68] J. Peterka, J. Cermak, L. Cochran, B. Cochran, N. Hosoya, R. Derickson, C. Harper, J. Jones and B. Metz, "Wind Uplift Model for Asphalt Shingles,"Journal of Architectural Engineering, vol. 3, no. 4.

[69] J. Koontz, "Shingle splitting problem," Western Roofing Magazine, 1990.

[70] T. Marshall, S. Morrison, R. Herzog and J. Green, "Wind Effects on Asphalt Shingles," Haag Engineering Co., Irving, TX, USA, 2010.

[71] T. Marshall, "Roof Damage Issues in Hurricanes," Haag Engineering Company, 2004.

[72] T. Marshall, "Curved Corner Fractures in Concrete Tile," Haag Engineering Company, 1990.

[73] Haag-Engineering, Field Guide to Residential Roof Damage Assessment, Haag Engineering Company, 2020.

[74] B. Bienkiewicz and Y. Sun, "Wind loading and resistance of loose-laid systems," Journal of Wind Engineering and Industrial Aerodynamics, vol. 72, no. 1, pp. 401-410, 1997.

[75] M. Noone and W. Blanchard, "Asphalt shingles — a century of success and improvement," in Tenth Conference on Roofing Technology, Gaithersburg, Maryland, USA, 1993.

[76] W. Cullen, "Research and performance experience of asphalt shingles," in 10th Conference on Roofing Technology, Gaithersburg, MD, USA, 1993.